Role of the Intermolecular Vibrations in the Hydrogen Transfer Rate: The 3-Methylindole−NH_3 Complex

Olivier David,[†] Claude Dedonder-Lardeux,*[,†] Christophe Jouvet,[†] and Andrzej L. Sobolewski[‡]

Laboratoire de Photophysique Moléculaire du CNRS, Bât. 210, Université Paris-Sud, 91405 Orsay, France, and Institute of Physics, Polish Academy of Sciences, PL-02668 Warsaw, Poland

Received: May 15, 2006

The lifetimes of the 3-methylindole−NH_3 complex have been measured on different vibronic levels involving intermolecular modes and decrease from 530 to 65 ps, in a mode specific manner. Geometry optimizations of the ground and excited states have been performed with ab initio methods, and as in the case of phenol and indole, a repulsive $\pi\sigma^*$ state lies close to the initially excited $\pi\pi^*$ state. From these calculations, it seems that both in-plane and out-of-plane vibrations induce a faster nonradiative decay.

Introduction

The electronically excited states of indole and substituted indoles have attracted considerable attention in the context of understanding the complex photophysical behavior of tryptophane (Trp) side chains in proteins. The fluorescence of Trp is highly sensitive to environment, making it an ideal choice for reporting protein conformation changes and interactions with other molecules.[1] The fluorescence quantum yield ranges from 0.35 to near zero.[2] The variation of the fluorescence lifetime of Trp or its indole chromophore has also been the subject of many investigations in both condensed and gas phases.[1,3−16] However, until recently, no clear picture had emerged from these works that allows us to understand why the fluorescence lifetime (or the fluorescence quantum yield) varies by more than 2 orders of magnitude, depending on the environment.

A simple and general mechanistic picture of nonradiative decay of biomolecules such as nucleic acid bases and aromatic amino acids has been suggested.[17] The key role in this analysis is played by an excited singlet state of $\pi\sigma^*$ character, which has repulsive potential-energy functions with respect to the stretching of OH or NH bonds. The $^1\pi\sigma^*$ potential-energy function intersects not only the bound potential-energy functions of the $^1\pi\pi^*$ excited states, but also that of the electronic ground state. These symmetry-forbidden intersections for the planar system are converted into conical intersections when out-of-plane modes are taken into account. Via predissociation of the $^1\pi\pi^*$ states and a conical intersection with the ground state, the $^1\pi\sigma^*$ state triggers an internal-conversion (IC) process. The lifetime of the optically excited $^1\pi\pi^*$ state is thus governed by the first intersection which determines the barrier for an IC process, and varies from one molecule to the other depending largely on the energy gap between the $^1\pi\sigma^*$ and the $^1\pi\pi^*$ states.

If a nearby molecule is linked to indole by hydrogen bond involving the H atom of the azine NH moiety, this hydrogen atom is transferred to the molecule due to electronic excitation, and the process removes the conical intersection with the ground state along the NH stretching coordinate. Indeed, excitation of indole−$(NH_3)_n$ clusters leads to a hydrogen transfer reaction and formation of $NH_4(NH_3)_n$ radicals.[14,15,18] Within an excess of a few tenths of an electronvolt, the reaction proceeds very quickly and operates in the 50 ps regime.[15] The strong hydrogen affinity of the ammonia molecule and its cluster are the important parameters for the observation of the H transfer process, and this process explains why the excited-state lifetime is short (sub-nanosecond) in indole−ammonia clusters as compared to all other clusters (water, methanol) where the lifetime is much longer.

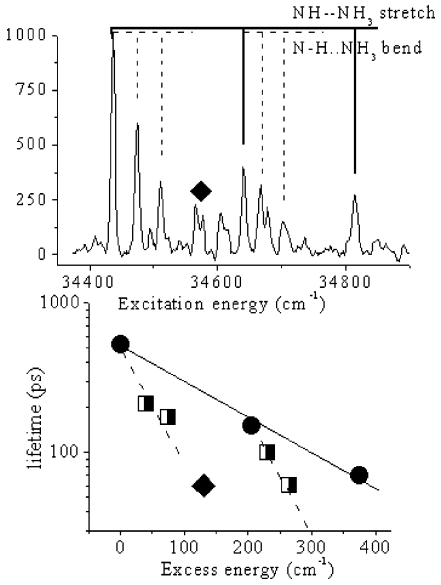

Figure 1. Vibronic levels and lifetimes of the 3-methylindole−NH_3 complex. Upper panel: R2PI excitation spectrum detecting the 3-methylindole−NH_3 ion signal (m/z = 148). Lower panel: excited-state lifetimes as a function of the excess vibrational energy.

To investigate the role of the vibration in the $\pi\pi^*/\pi\sigma^*$ coupling, we have measured the lifetime of different intermolecular vibrations of the 3-methylindole−NH_3 complexes. This system was chosen since it is the simplest indolic derivative which is similar to tryptophan, i.e., with an alkyl substituent in the C3 position, and the hydrogen transfer reaction has been characterized in the excited state of 3-methylindole−$(NH_3)_n$ clusters by observation of the $NH_4(NH_3)_n$ radicals[18] and by the

* To whom correspondence should be addressed. E-mail: claude.dedonder-lardeux@ppm.u-psud.fr.
† Université Paris-Sud.
‡ Polish Academy of Sciences.

10.1021/jp062950y CCC: $33.50
Published on Web 07/12/2006

extinction of the hydride stretch infrared band.[19] The ground $\pi\pi$ and excited $\pi\pi^*$ states are of a′ symmetry while the $\pi\sigma^*$ state belongs to symmetry representation a″ when the C_s symmetry of the molecule is preserved. As in the phenol−NH_3 complex where the intermolecular stretching vibration accelerates the hydrogen transfer reaction,[20,21] the coupling between the $\pi\pi^*$ and $\pi\sigma^*$ states is expected to be very sensitive to the vibrational excitation of the former state. To assign the 3-methylindole−NH_3 vibrational spectrum, ab initio calculations have been performed including optimization of the ground and the first excited states and calculation of vibrational frequencies.

Experimental Section

3-Methylindole−ammonia clusters are produced by expanding a mixture of NH_3 and pyrrole seeded in helium through a pulsed valve. The gas mixture is obtained by passing the premixed He/NH_3(0.5−2%) gas flow over a reservoir containing 3-methylindole heated at 45 °C. The backing pressure is varied between 0.5 and 3 bar, and the nozzle diameter is 300 μm. The jet is skimmed before entering the time-of-flight mass spectrometer (Jordan Co), between the extraction electrodes where the clusters are ionized. The ions are then accelerated between two other electrodes before flying in the 1 m field free region (grounded). The ions are detected by microchannel plates, and the signal is amplified and recorded on a LeCroy 9400 oscilloscope.

The mass spectrometer can also be run in reflectron mode when high resolution mass spectra are necessary: in that case, after the 1 m field free region, the ions are reflected by a series of electrodes and fly another 1 m before being detected by a second pair of microchannel plates.

Often in multiphoton ionization spectroscopy of clusters containing aromatic molecules and NH_3,[23] some evaporation occurs after ionization. One can get this evaporation information using a pulsed extraction as done in the case of naphthol−NH_3.[18,22]

In this method, a long waiting time between the excitation/ionization lasers and the ion extraction pulses is set in order to let the initially produced ion cloud expand if some kinetic energy is released in the reaction. This method is sensitive to the dispersion of the ion cloud along the TOF axis, in our case the vertical axis. The ions which will be located near the lower electrode are more accelerated than the ones near the upper one; they will travel faster in the field free region of the TOF and will arrive on the detector at earlier times. Practically, when the delay between the laser and the extracting field is increased, the excitation/ionization position between the two extraction plates is varied by translating the lens upstream of the jet axis so that the ions can reach the detector. To get rid of the initial width of the mass peaks, due to the finite size of the laser beams and to the distribution of velocities in the jet, the variation of the peak width (Δw) can be measured as a function of the delay (Δt) between laser and pulsed extraction field: there is a linear variation of Δw versus Δt, and the resulting slope, divided by a calibration parameter, gives a direct measure of the velocity. In the pulsed extraction mode, the mass spectrometer works in the direct mode, and high voltages (1000 and 750 V) are switched on the lower and upper extraction electrodes with a Behlke high voltage switch.

For time-resolved experiments, a homemade picosecond OPO laser system was used.[21] The picosecond pulses are produced with a Nd:YAG laser through a combination of saturable absorber and passive negative feedback; a macroimpulsion involving 50 pulses of 10 ps duration, separated by 10 ns, is produced at a 20 Hz repetition rate. Seventy percent of the 1.064 μm pump power, e.g., 800 mW, is frequency tripled to 355 nm (220 mW) to pump synchronously a BBO-based visible OPO laser tunable from 410 to 750 nm. The present experiment makes use of the latter visible OPO output around 575 nm which is further frequency doubled to excite the S_0–S_1 transition. A portion of the 355 nm pump laser is optically delayed and used as the ionization probe laser. The spectral width of the visible OPO is less than 3 cm^{-1}. The laser characteristics make it possible to monitor dynamical processes with a resolution of 10 ps, if the reactive system can relax within 10 ns corresponding to the laser pulse separation. The multipulse structure precludes, however, to measure the rise time of stable reaction products.

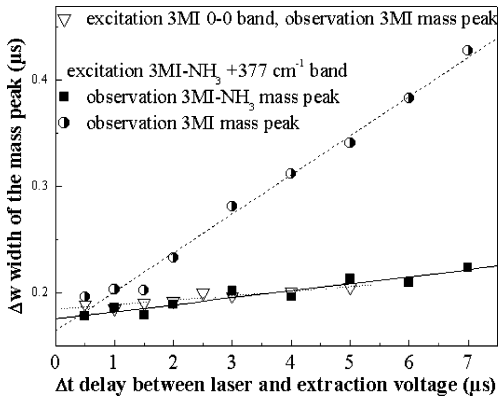

Figure 2. Variation of the peak widths Δw as a function of the delay between ionization laser and pulsed extraction voltage Δt. õ Open triangles and dotted line: excitation of the free 3-methylindole molecule (3MI) on its 0−0 transition at 34 882 cm^{-1}; the mass peak width stays narrow since no evaporation process occurs. Solid squares and full line: excitation of the 3-methylindole−NH_3 complex (3MI−NH_3) on the +377 cm^{-1} band and observation on the 3-methylindole−NH_3 complex mass peak (m/z = 148); the peak stays narrow indicating the absence of evaporation process. Half-filled circles and dashed line: excitation of the 3-methylindole−NH_3 complex on the +377 cm^{-1} band and observation on the 3-methylindole monomer mass peak (m/z = 131); the peak broadens since the complex has lost the ammonia moiety.

Results

The excitation spectrum recorded for the 3-methylindole−ammonia complex (1−1) on Figure 1 consists of a series of vibrational bands starting at −440 cm^{-1} from the 0−0 transition of the bare molecule. The three first bands had already been observed,[8] and for the other bands, the broadening of the mass peaks as a function of the delay between the laser and the extraction voltage has been measured to see if they come from this 1−1 complex or from larger clusters that would have evaporated one or more ammonia molecules.

As can be seen on Figure 2, when we set the wavelength on a particular vibrational band (+377 cm^{-1} in Figure 1), we can record the ion signal either on the 1−1 complex mass peak or on the bare molecule mass peak. In the former case, the broadening measured on the 1−1 mass peak as a function of the delay between the laser and the extraction voltage is small and is the same as the broadening measured for the band origin of the bare molecule, indicating that there is no kinetic energy in the ion observed, i.e., no evaporation. On the contrary, when the 1−1 complex is excited and the ion signal of the molecule is recorded, we measure a much greater broadening, as expected since the complex has evaporated to be observed on the bare molecule mass channel. All the bands of the 1−1 complex

TABLE 1: Lifetime of the 3-Methylindole−NH_3 Complex as a Function of the Excited Vibronic Level

relative band position from the 0−0 transition[a] (cm^{-1})	lifetime (ps)	assignment[b]
0	530 ± 20	0−0
39	205 ± 10	1 quantum N−H···NH_3 bend
75	172 ± 10	2 quanta N−H···NH_3 bend
130	63 ± 6	indole out of plane deformation or NH_3 torsion
205	145 ± 11	1 quantum N−H···NH_3 stretch
229	100 ± 6	1 quantum N−H···NH_3 stretch + 1 quantum N−H···NH_3 bend
268	59 ± 5	1 quantum N−H···NH_3 stretch + 2 quanta N−H···NH_3 bend
377	65 ± 5	2 quanta N−H···NH_3 stretch

[a] Transition origin at 34 442 cm^{-1}. [b] Tentative assignment from theoretical calculations of the excited-state frequencies (see discussion in text).

shown in Figure 1 present the same small broadening and can then be assigned to the 1−1 complex.

The lifetimes of the complex have been measured on the different bands by scanning the optical delay line and are reported in the lower panel of Figure 1 and in Table 1. The lifetime has a tendency to decrease with the excitation energy but in a nonmonotonic way: when the excess energy is 205 cm^{-1} the lifetime is longer than when the excess energy is 130 cm^{-1}. The variation of the lifetime is then highly dependent on the excited vibrational levels.

Theoretical Calculations

All calculations have been performed with the Turbomole program package (V.5.7).[23]

a. Ground State. The ground-state structures and vibrational modes have been calculated by three different theoretical methods implemented in Turbomole: the RI-DFT/B-P86 method (resolution-of-the-identity approximation with the B-P86 functional)[24,25] with the triple-ζ valence plus polarization (TZVP) basis sets, and with DFT/B3LYP and RI-MP2 methods using the same basis set.

The ground state has been optimized at the RI-MP2 (TZVP) level keeping the system planar or breaking the C_s symmetry by out of plane distortion of the NH···NH_3 moiety by 30°. Two minima on the potential-energy (PE) surface of the ground state have been found; the lowest corresponds to a slightly nonplanar geometry with the NH group distorted by 13° out of the molecular plane (Figure 3a), and the other one, slightly higher in energy (0.05 eV, 390 cm^{-1}), is planar (Figure 3b). In both cases, the angle and distances are very similar to those reported by A. Combs et al. using the 6-311++G** basis set for the 3-methylindole geometry, except for the pyrrolic NH distance which is elongated by the hydrogen bonding with the ammonia molecule.[26] The structure optimized with DFT is also planar with a similar equilibrium geometry.

The most characteristic low-frequency vibrational modes calculated with the three different methods are collected in Table 2. All three theoretical methods give similar results except for the NH_3 pseudorotation in the ground state (torsion around the NH···N axis) which is substantially lower at the MP2 level.

b. Excited States. The vertical energies of electronically excited states have been calculated starting from both ground-state equilibrium geometries using the RI-CC2/cc-pVDZ method with additional diffuse functions (aug-cc-pVDZ) on carbon and nitrogen atoms. For both the planar and slightly bent geometries, the results are similar: The $S_1(\pi\pi^*)$ state is found at 4.65 eV, the S_2 ($\pi\pi^*$) state at 4.79 eV, and the S_3 ($\pi\sigma^*$) at 4.84 eV when starting from the nonplanar geometry and 4.65, 4.81, 4.82 eV for the C_s geometry. In the free molecule, at the same theoretical level, these states are found at 4.76, 4.87, and 4.87 eV, respectively, and there is no essential change of the relative energy of the states upon complexation.

The optimization of the first excited state has been done starting from a nonplanar geometry of the ground state. The final equilibrium geometry is stabilized by 0.48 eV as compared to the vertical energy. Its structure is characterized by a shortening of the NH···NH_3 distance by 0.12 Å and an in-plane bending of the NH···NH_3 angle from linear in the ground state to 160° in S_1 (Figure 4a). In this nonconstrained geometry optimization, the NH_3 molecule comes back in the indole plane, and the optimization of the excited state under C_s symmetry leads to a similar geometry (Figure 4b). The S_0-S_1 electronic transition is at 4.17 eV, which can be compared with the experimental 0−0 transition at 4.27 eV.

It should also be mentioned that, in C_s symmetry, the optimization of the first state of a″ symmetry ($\pi\sigma^*$) results in a geometry where the pyrrolic H atom is transferred from the 3-methylindole to the NH_3 molecule (see Figure 5) as calculated previously in the case of the indole−NH_3 complex.[3] The energy of the H-transferred structure in the $\pi\sigma^*$ state is 1.62 eV higher

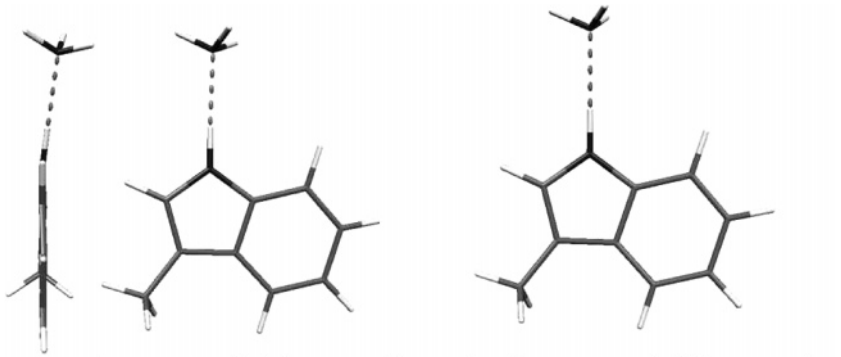

Figure 3. Ground-state RI-MP2 optimization: (a) nonplanar equilibrium geometry, the ammonia molecule is out of plane by 13°; (b) C_s equilibrium geometry. In both geometries, the NH···N(H_3) angle is 180°, the pyrrolic NH distance is 1.022 Å (0.016 Å longer than in the free molecule), and the hydrogen bond NH···NH_3 is 1.984 Å.

TABLE 2: Calculated Vibrational Frequencies in the Ground and Excited States and Tentative Assignment of the Experimental Bands[a]

vibrational frequencies (cm^{-1})	ground state DFT/B3LYP[b]	ground state RI-DFT[c]	ground state RI-MP2[c]	excited state RI-CC2[d]	expt
NH_3 pseudorotation	40	47	12	83	130?
NH_3 bend out-of-plane	41	41	41	32	
NH_3 bent in-plane	43	45	34	53	39
CH_3 pseudorotation	123	116	118	75	
indole out-of-plane deformation	158	150	145	114/140	130?
NH_3–H stretch	160	154	153	182	205
CH_3 bend in plane	225	221	223	218	
3-methylindole-NH_3 bend in-plane	228	215	208	313	
3-methylindole-NH_3 bend out-of-plane	259	274	257	189-285	

[a] See text. [b] Basis set 6-31G**. [c] Basis set TZVP. [d] Basis set cc-pVDZ on hydrogen atoms and aug-cc-pVDZ on nitrogen and carbon atoms.

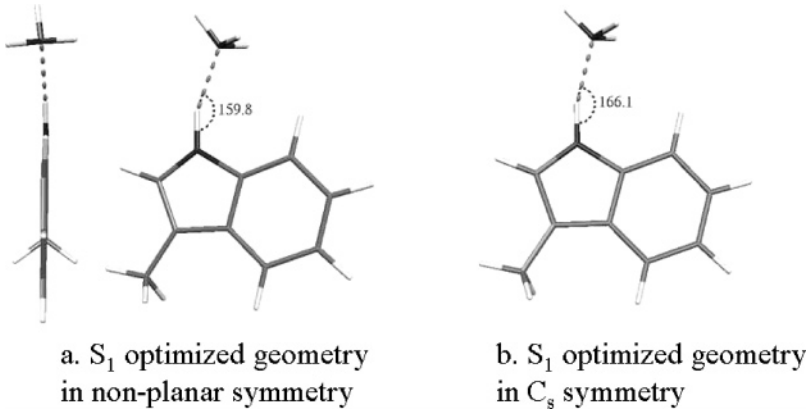

Figure 4. First excited state (S_1) optimization (RI-CC2 method): (a) nonplanar symmetry, the ammonia molecule is less out-of-plane than in the starting ground-state geometry; (b) C_s geometry optimization. In both cases, the NH···NH_3 distance is shorter than in the ground state by 0.12 Å and the ammonia molecule bends in plane toward the six membered ring.

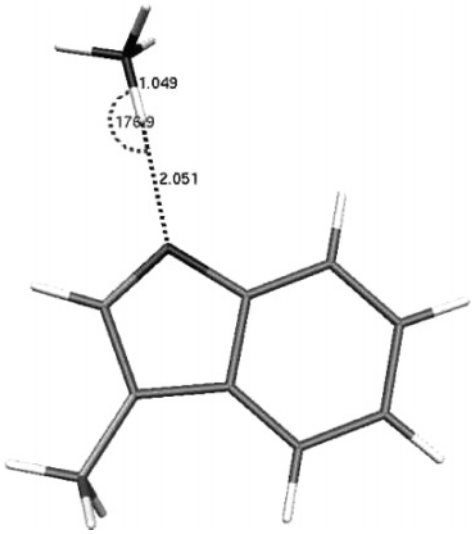

Figure 5. Geometry optimization of the first state of a″ symmetry ($\pi\sigma^*$ state).

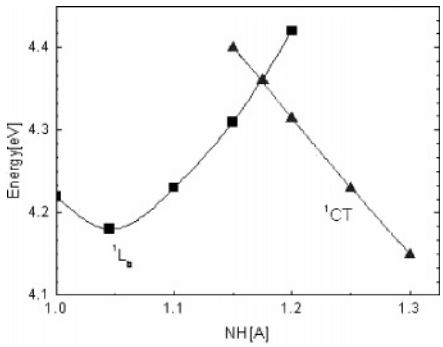

Figure 6. Excited-state potential energy functions calculated using the coordinate-driven minimum-energy-path (CD-MEP) approach. For each value of the NH distance, all remaining coordinates are optimized. Squares: first excited state ($\pi\pi^*$ ^1L_b) in nonplanar symmetry. Triangles: excited state of a″ symmetry ($^1\pi\sigma^*$ charge transfer state or ^{1}CT state) in C_s geometry.

than the ground-state energy (at this geometry), which itself is 2.25 eV higher than the optimized ground state. The total energy of the optimized $\pi\sigma^*$ state is then 3.86 eV above the optimized ground-state energy, i.e., 0.31 eV lower than the adiabatic energy of the $S_1(\pi\pi^*)$ state energy (4.17 eV). One can deduce from these results that the $\pi\sigma^*$ state crosses the first excited $\pi\pi^*$ state along the hydrogen transfer reaction coordinate. This result is quite similar to that obtained for the phenol−NH_3 complex[27] where, along the H transfer coordinate, the $\pi\sigma^*$ state crosses the first $\pi\pi^*$ state but not the ground state.

The reaction path for the hydrogen atom transfer to the ammonia was calculated using the coordinate-driven minimum-energy-path (CD-MEP) approach; i.e., for a given value of the NH distance, all remaining coordinates were optimized (Figure 6). The energy at the crossing point between the $\pi\pi^*$ and $\pi\sigma^*$ states is rather low (0.18 eV above the minimum of the $\pi\pi^*$ state). We were expecting to gather evidence indicating an avoided crossing around $R_{NH} = 1.175$ Å from which we could deduce the coupling between the $\pi\pi^*$ and $\pi\sigma^*$ states, but it is not the case, which indicates a strong curvature of the excited-state PE surface near the $\pi\pi^*/\pi\sigma^*$ intersection along coordinates other than the NH stretch considered here.

The excited state ($\pi\pi^*$) vibrational frequencies calculated at the minimum of the S_1 state are presented in Table 2 in comparison with the ground-state frequencies. Some vibrational modes exhibit a strong frequency change between the ground and the excited states, in particular, the NH_3 pseudorotation

which is higher in the excited state than in the ground state. This effect corresponds to an increase of the torsional barrier that may be due to the shortening of the distance between NH_3 and the C−H bond on the six-membered ring.

Discussion

According to the Franck−Condon (FC) principle, the most active modes in the excitation spectrum should be those for which the geometry change between the ground and excited state is the largest. The calculated equilibrium geometries of the S_0 and S_1 states indicate the greatest changes for the NH···N distance and for the angle of the pyrrolic NH bond in plane toward the six-membered ring. Therefore, the NH···NH_3 bending and the N−H···NH_3 stretching should be the most FC active mode in the spectrum. The low-frequency progression of 39 cm^{-1} associated with the 0−0 transition and with the +205 cm^{-1} band is thus assigned to the bending (in-plane bending calculated at 53 cm^{-1} in the excited state at the RI-CC2 level) while the bands at 205 and 377 cm^{-1} are assigned to the first and second members of a stretching progression (calculated frequency of 182 cm^{-1}). The band at 130 cm^{-1} is less straightforward to assign. It can be assigned to an indole out-of-plane deformation or to the ammonia torsion (calculated at 114 and 82 cm^{-1}, respectively).

Using this assignment, the lifetime decreases with the excitation of the NH−N intermolecular stretching coordinate, from 530 ps for the 0−0 transition, to 145 ps for one quanta and 65 ps for two quanta. Such a shortening of the lifetime with excitation energy has already been observed in the case of the phenol−NH_3 complex.[20,21,28]

The 130 cm^{-1} vibration also presents a shortened lifetime of 65 ps as can be expected if out-of-plane deformations are involved leading to an increase of the $\pi\pi^*/\pi\sigma^*$ coupling, but this does not allow us to discriminate between the butterfly motion and the NH_3 torsion.

The nonradiative decay is accelerated by the 39 cm^{-1} progression, which we tentatively assign to the in-plane bending of the ammonia molecule, while we were expecting out-of-plane vibrations to mix the bright $\pi\pi^*$ and the dark $\pi\sigma^*$ states.

It should be stressed that the calculations performed indicate that the shortening of the lifetime in the complex is not simply due to a smaller $\pi\pi/\pi\sigma^*$ energy gap. Indeed, as long as one can trust these calculations, the $\pi\pi^*/\pi\sigma^*$ energy gap does not change from the isolated molecule to the complex whereas the lifetime changes drastically.[8,11] It is clearly a problem that ab initio calculations cannot solve, since dynamics at the conical intersection are quite subtle. These measurements might be useful as experimental values to test wave packet propagations methods necessary to give a good answer to the dynamical problem.

In any event, the experiment shows that the lifetime of the 3-methylindole−ammonia complex is strongly dependent upon vibronic excitation within the S_1 state, and this particularly concerns the intermolecular NH···NH_3 modes. This means that one should be very cautious in the interpretation of the femtosecond experiments on indole clustered with ammonia, in which the laser width does not allow selective excitation.[29−31]

Conclusions

The lifetime of the first excited state in the 3-methylindole−NH_3 complex is strongly dependent on the intermolecular vibration. As experimentally observed, the excitation of NH···N stretching coordinate is expected to favor the H transfer reaction. High level ab initio optimization of the equilibrium geometry of the S_1 state and calculated vibrational frequencies compared with the experimental observations seem to indicate that the in-plane bending vibration also favors the H transfer from the aromatic chromophore (3-methylindole) to the solvent (ammonia).

Acknowledgment. This work has been supported by a CNRS/PAN cooperation agreement (grant 11887).

References and Notes

(1) Lakowicz, J. R. *Principles of Fluorescence Spectroscopy*, 2nd ed.; Kluwer Academic/Plenum: New York, 1999.

(2) Chen, Y.; Barkley, M. D. *Biochemistry* **1998**, *37*, 9976.

(3) Sobolewski, A. L.; Domcke, W. *Chem. Phys. Lett.* **2000**, *329*, 130.

(4) Pailthorpe, M. T.; Nicholls, C. H. *Photochem. Photobiol.* **1971**, *14*, 135.

(5) Britten, A. Z.; Lockwood, G. *Spectrochim. Acta* **1976**, *32*, 1335.

(6) Mialocq, J. C.; Amouyal, E.; Bernas, A.; Grand, D. *J. Phys. Chem.* **1982**, *86*, 3173.

(7) Petrich, J. W.; Chang, M. C.; McDonald, D. B.; Flemming, G. R. *J. Am. Chem. Soc.* **1982**, *105*, 3824.

(8) Hager, J. W.; Demmer, D. R.; Wallace, C. S. *J. Phys. Chem.* **1987**, *91*, 1375.

(9) Lipert, R. J.; Bermudez, G.; Colson, S. D. *J. Phys. Chem.* **1988**, *92*, 3801.

(10) Demmer, D. R.; Leach, G. W.; Outhouse, E. A.; Hager, J. W.; Wallace, S. C. *J. Phys. Chem.* **1990**, *94*, 582.

(11) Arnold, S.; Sulkes, M. *J. Phys. Chem.* **1992**, *96*, 4768.

(12) Peon, J.; Hess, G. C.; Pecourt, J. L.; Yuzawa, T.; Kohler, B. *J. Phys. Chem. A* **1999**, *103*, 2460.

(13) Short, K. W.; Callis, P. R. *J. Chem. Phys.* **2000**, *113*, 5235.

(14) Dedonder-Lardeux, C.; Grosswasser, D.; Jouvet, C.; Martrenchard, S. *PhysChemComm* **2001**, 1.

(15) Lippert, H.; Stert, V.; Hesse, L.; Schulz, C. P.; Radloff, W.; Hertel, I. V. *Eur. Phys. J. D* **2002**, *20*, 445.

(16) Fender, B. J.; Sammeth, D. M.; Callis, P. R. *Chem. Phys. Lett.* **1995**, *239*, 31.

(17) Sobolewski, A. L.; Domcke, W.; Dedonder-Lardeux, C.; Jouvet, C. *Phys. Chem. Chem. Phys.* **2002**, *4*, 1093.

(18) David, O.; Dedonder-Lardeux, C.; Jouvet, C. *Int. Rev. Phys. Chem.* **2002**, *21*, 499.

(19) Dian, B. C.; Longarte, A.; Zwier, T. S. *J. Chem. Phys.* **2003**, *118*, 2696.

(20) Ishiuchi, S.; Daigoku, K.; Saeki, M.; Hashimoto, K.; Sakai, M.; Fujii, M. *J. Chem. Phys.* **2002**, *117*, 7077.

(21) Gregoire, G.; Dedonder-Lardeux, C.; Jouvet, C.; Martrenchard, S.; Peremans, A.; Solgadi, D. *J. Phys. Chem. A* **2000**, *104*, 9087.

(22) Dedonder-Lardeux, C.; Grosswasser, D.; Jouvet, C.; Martrenchard, S.; Teahu, A. *Phys. Chem. Chem. Phys.* **2001**, *3*, 4316.

(23) Ahlrichs, R.; Bar, M.; Haser, M.; Horn, H.; Kolmel, C. *Chem. Phys. Lett.* **1989**, *162*, 165.

(24) Arnim, M.; Ahlrichs, R. *J. Comput. Chem.* **1998**, *19*, 1746.

(25) Bauernschmitt, R.; Haser, M.; R., T.; Ahlrichs, R. *Chem. Phys. Lett.* **1997**, *264*, 573.

(26) Combs, A.; McCanna, K.; Autreya, D.; Laanea, J.; Overmanb, S. A.; Thomas, G. J. J. *J. Mol. Struct.* **2005**, *735−736*, 271.

(27) Sobolewski, A. L.; Domcke, W. *J. Phys. Chem. A* **2001**, *105*, 9275.

(28) Ishiuchi, S.; Sakai, M.; Daigoku, K.; Tadashi, U.; Yamanaka, T.; Hashimoto, K.; Fujii, M. *Chem. Phys. Lett.* **2001**, *347*, 87.

(29) Lippert, H.; Stert, V.; Hesse, L.; Schulz, C. P.; Hertel, I. V.; Radloff, W. *Chem. Phys. Lett.* **2003**, *371*, 208.

(30) Lippert, H.; Stert, V.; Hesse, L.; Schulz, C. P.; Hertel, I. V.; Radloff, W. *J. Phys. Chem. A* **2003**, *107*, 8239.

(31) (31)Lippert, H.; Stert, V.; Schulz, C. P.; Hertel, I. V.; Radloff, W. *Phys. Chem. Chem. Phys.* **2004**, *6*, 2718.